Int J Adv Manuf Technol (2015) 76:1793–1805
DOI 10.1007/s00170-014-6394-2

ORIGINAL ARTICLE

Modelling residual stresses in friction stir welding of Al alloys—a review of possibilities and future trends

Jesper H. Hattel · M. R. Sonne · Cem C. Tutum

Received: 4 April 2011 / Accepted: 15 September 2014 / Published online: 26 September 2014

Abstract Residual stresses are very important in any joining process of materials since they act as pre-stresses in the loading situation of the joint, thereby affecting the final mechanical performance of the component. This is also the case for friction stir welding (FSW) which is a complex solid-state joining process characterized by a pronounced multiphysical behaviour involving phenomena such as change of temperature, material flow, change of microstructures and formation of residual stresses. Thus, models of FSW are typically divided into thermal models, flow models, residual stress models and microstructural models where the classification of the model normally originates from its purpose rather than from the modelling discipline applied. In the present paper, the focus is on presenting and classifying the most important residual stress models for FSW of aluminium alloys in terms of their background, numerical framework and application as well as putting them into proper context with respect to some of the new trends in the field, e.g. coupling with subsequent load analyses of the in-service situation or applying residual stress models of FSW in numerical optimization.

Keywords Friction stir welding · Residual stress · Numerical modelling · Thermomechanics

J. H. Hattel (✉) · M. R. Sonne
Department of Mechanical Engineering, Section of Manufacturing Engineering, Technical University of Denmark, building 425, 2800 Kgs. Lyngby, Denmark
e-mail: jhat@mek.dtu.dk

C. C. Tutum
Department of Electrical and Computer Engineering, MichiganStateUniversity, Egineering Bldg. 428 S Shaw LN Room 2120, 48824 East Lansing, MI, USA

1 Introduction

Friction stir welding (FSW) is an efficient solid-state joining technique intended for joining of e.g. similar or dissimilar high-strength aluminium alloys, which are difficult to weld with traditional welding techniques. Some of the advantages of the FSW method are improved mechanical properties of the welds, reduced distortions, somewhat lower residual stresses and benign environmental characteristics [1].

The FSW process, shown schematically in Fig. 1a, utilizes a spinning tool consisting of a pin and a shoulder, which is plunged into the metal sheet to be welded and forced forward along the weld line to create a joint. During the welding process, heat is generated due to the friction between the tool and the workpiece, as well as due to the severe plastic deformation of the material. The heat conducted into the workpiece influences the quality of the weld in terms of (i) significant changes in the weld material properties, (ii) build-up of residual stresses and (iii) distortion of the welded part, with all these three phenomena obviously being interrelated.

Because of the relatively low heat generation in the FSW process, it is generally believed that residual stresses are low; however, due to the non-uniform heating as well as the very rigid clamping arrangement needed in the process, considerable residual stresses can be found in FSW welds [2–6] and sometimes at a level of the base material yield strength [7]. Figure 1b shows typical longitudinal and transversal residual stress fields in the FSW joint, from Feng et al. [18]. It is very obvious that residual stresses will influence the subsequent mechanical behaviour of the structure since they act as pre-stresses during the in-service loading. This might lead to stresses exceeding the yield limit just during static loading [8], but also reduce fatigue strength [9, 10] or highly influence the buckling behaviour [11, 12]. Thus, many contributions have been given in literature for measuring and calculating residual stresses in FSW. Regarding experimental measurements, application of non-destructive

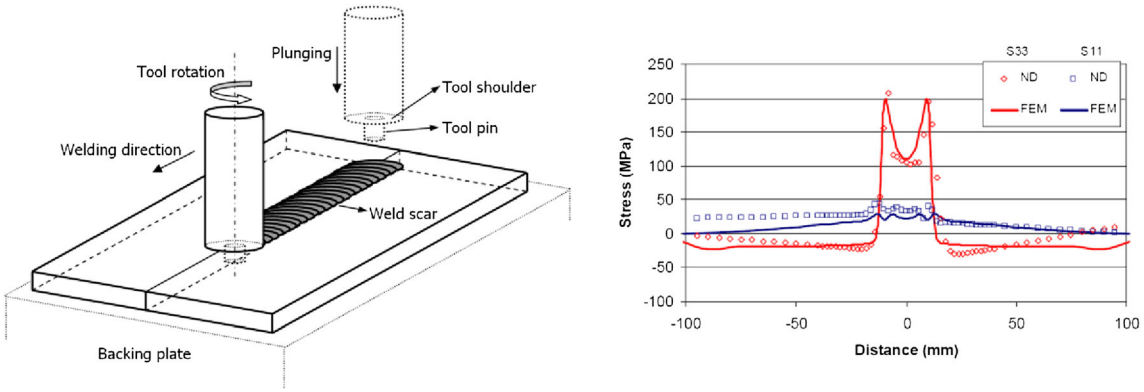

Fig. 1 **a** Schematic view of the FSW process. **b** Typical distribution of residual longitudinal (*s33*, *red*) and transversal (*s11*, *blue*) normal stresses across a FSW AL6061-T6 weld joint (*ND* neutron diffraction measurements), 787 mm/min (13.12 mm/s), 1250 rpm. From Feng et al. [18]

methods like X-ray diffraction [3, 5, 13–16] and neutron diffraction [17, 18] can be found as well as destructive methods like cut-compliance [19, 20] and the contour method [21]. In this context, it is very important to emphasize that measuring residual stresses of FSW normally involves cutting out a test piece of the real welded structure, thus leading to potential relaxation of residual stresses [64]. For this reason, Threadgill and coworkers [22] state that a weld length of approximately eight times the diameter of the tool must be retained if 90 % of the residual stresses are to be retained when cutting out the test piece and argue that not meeting this criterion might be the explanation for the low residual stresses found in some experimental studies in literature [3, 23]. The state of the art in measuring stresses for FSW involves in situ ND measurements during the welding process [24, 25] (thereby also avoiding cutting out test pieces), thus being able to follow the evolution of transient stress fields into the final residual stress field.

Many contributions regarding modelling of residual stresses in FSW have been given in literature [8, 18, 26–34, 50–57], and common for them all is that they somehow predict the thermally induced stresses arising from the welding process. Some models only consider the rotating tool as a moving heat source [8, 18, 26–34] whereas others take the coupling between the temperatures and the material flow into account [50–57]. All models take the thermal softening into account; however, while some just employ a temperature-dependent yield strength, others apply metallurgical models of varying complexity for predicting the evolution of e.g. hardness and thereby yield strength. These issues will be addressed more thoroughly in specific sections of the paper which is structured as follows. First, a short overview of modelling of FSW and a description of the mandatory thermal models for modelling residual stresses in FSW are given. This is followed by a brief description of metallurgical models for the evolution of mechanical properties. The most common type of models for residual stresses in FSW, namely thermomechanical models neglecting the flow, is then presented and followed by the more complex thermomechanical models, which take the flow into account. Finally, the means of reducing residual stresses in FSW joints, coupling of residual stress models with models for subsequent loading during in-service as well as optimization studies of FSW based on residual stress modelling are discussed.

2 Modelling of FSW

FSW is a process which is characterized by a complex multiphysics behaviour. During the plunging, dwelling and traversing of the tool, the material flow, the resulting temperatures and the microstructural evolution in essence will be closely coupled; see Fig. 2 (left). It is important to emphasize that transient stresses will be produced already during this phase. Apart from the direct effects on the resulting microstructures and mechanical properties from the stirring motion and heating during rotation and traversing of the tool, once the welding has terminated and the parts cool down, the temperature fields also affect microstructures and thereby mechanical properties and these together with the thermal gradients and the clamping conditions give rise to transient and residual stresses in a semi-coupled way as shown in Fig. 2 (middle). As discussed earlier, these properties and stresses will in turn highly influence the mechanical performance of the part during the in-service loads; see Fig. 2 (right).

In general, models for FSW are categorized by either their area of application, i.e. flow models or residual stress models, or by the continuum mechanics approach they are based upon, i.e. computational solid mechanics (CSM) models or computational fluid dynamics (CFD) models, where the former typically are Lagrangian and the latter Eulerian; see Fig. 3.

The equations for conservation of momentum, energy and mass, respectively, are in the Lagrangian and Eulerian frames given in Table 1. These fundamental, governing partial differential equations depending on the continuum mechanical

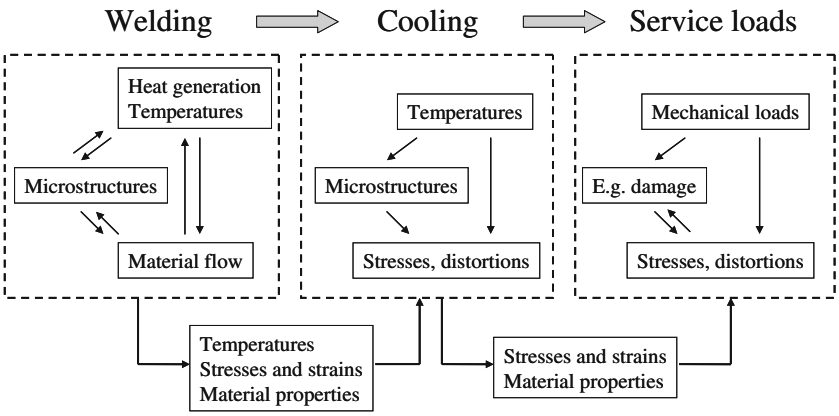

Fig. 2 The major modelling couplings in FSW during welding, cooling and loading. From Hattel et al. [35]

framework used will need to be modified and combined with proper constitutive laws for the particular case at hand. This will be done in the following with the particular purpose of modelling residual stresses in FSW and discussed in relation to the different numerical approaches available.

3 Thermal models for FSW

Any residual stress model of FSW will contain a model for calculating the temperatures. The core part of any such thermal model is how the heat generation from the rotating tool is described and applied as either a boundary condition for, or a source term in, the energy equation, be it in a Lagrangian or Eulerian frame; see Table 1. If a fully coupled thermomechanical model is used, access to the material flow/deformation fields as well as the formation of the shear layer will be available and this information will be reflected in the dissipation source term $\eta s_{ij}\dot{\varepsilon}_{ij}^{pl}$ in the two versions of the energy equation in Table 1.

However, for the semi-coupled thermomechanical models where material flow is not considered (which by far are the most frequent ones in literature), the procedure is normally to apply a surface heat flux as representing the entire heat generation, thereby avoiding the source term in the energy equation, which calls for knowledge about the material flow. Several suggestions in literature are given for the surface heat flux formulation (see [37, 38] for a detailed description), but common for them all is the need for "calibration" parameters. If one has access to an experiment from which it is possible to obtain the total heat generation from the measurements, one can use the well-known expression given in Eq. (1) to obtain the surface flux

$$\frac{q_{\text{total}}(r)}{A} = \frac{3Q_{\text{total}}r}{2\pi R_{\text{shoulder}}^3} \tag{1}$$

If you have information about the friction coefficient and the total downward force from the tool, and you assume full sliding, you can express the total heat generation as [79]

$$Q_{\text{total}} = \frac{2}{3}\pi\omega R_{\text{shoulder}}^3 \mu p \tag{2}$$

Either way, you need experimental information, and the most utilized procedure for evaluating the total heat generation is typically to perform the actual welds and measure it with a dynamometer, thereby accepting the inherent limitation of the resulting thermal model to predicting only temperatures

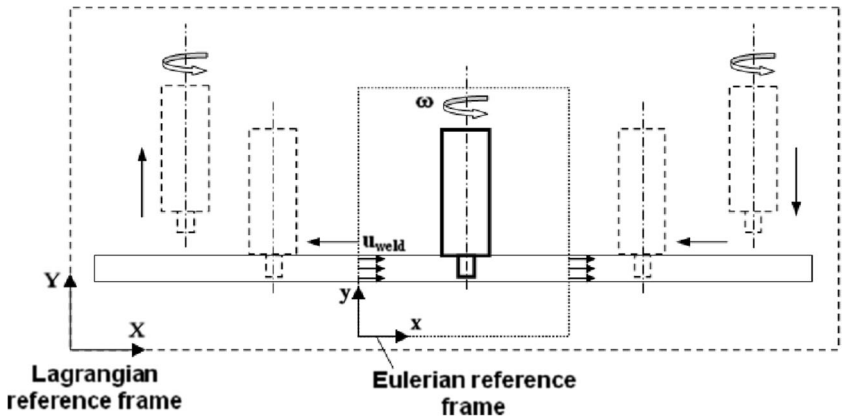

Fig. 3 Lagrangian frame (fixed coordinate system) and Eulerian frame (moving coordinate system) for modelling FSW [36]

Table 1 Governing equations for conservation of momentum, energy and mass, respectively, in Lagrangian and Eulerian frames [35]

Lagrangian frame Typically CSM	Eulerian frame Typically CFD
Energy	
$\rho c_p \dot{T} = \left(kT_{,i}\right)_{,i} + \eta s_{ij}\dot{\varepsilon}_{ij}^{pl}$	$\rho c_p \dot{T} = \left(kT_{,i}\right)_{,i} + \eta s_{ij}\dot{\varepsilon}_{ij}^{pl} - \mu_i\left(\rho c_p T\right)_{,i}$
Momentum	
$\rho \ddot{u}_i = \sigma_{ji,j} + p_i$	$\partial(\rho \dot{u}_i)/\partial t = \sigma_{ji,j} + p_i - \rho\left(\dot{u}_j \dot{u}_i\right)_{,j}$
Mass	
No explicit equation	$\dot{\rho} = -(\rho u_i)_{,i}$

for a *known* total heat generation. As a way to overcome this problem, Schmidt and Hattel [38] proposed a somewhat different thermal model in which the heat generation again is expressed as a surface heat flux from the tool shoulder (without the tool probe) into the workpiece, however being a function of the tool radius and the temperature-dependent yield stress as follows:

$$\frac{q_{\text{surface}}}{A}(r,T) = \omega r \tau(T) = \left(\frac{2\pi n}{60}\right) r \frac{\sigma_{\text{yield}}(T)}{\sqrt{3}}, \quad \text{for } 0 \le r \le R_{\text{shoulder}} \tag{3}$$

where n is the tool revolutions per minute, r is the radial position originating in the tool centre, R_{shoulder} is the tool shoulder radius and $\sigma_{\text{yield}}(T)$ is the temperature-dependent yield stress which approaches zero at the cut-off temperature (typically taken as the solidus temperature of the weld material) such that once the temperature approaches this value, the "self stabilizing effect" causes the heat source to "turn itself off", i.e. the material loses all its resistance, and the heat generation decreases automatically due to thermal softening. The model is often denoted "thermal-pseudo-mechanical" [38] since the heat generation is expressed via the temperature-dependent yield stress, thus taking some mechanical effects into account; however, it should be underlined that the model is a purely thermal model involving a temperature-dependent heat generation and in that sense it also uses a calibration parameter like the more conventional procedure in Eqs. (1) and (2). Obviously, this adds a non-linearity to the thermal model, meaning that the calculation time is increased by roughly a factor of two as compared to other thermal models where the heat source is prescribed itself, like in Eq. (1). It should be mentioned that both of the well-accepted expressions in Eqs. (1) and (2) can be directly derived from the more general formulation of analytically modelling the heat source in FSW given by Schmidt and Hattel in [39] which in essence results in the following equation:

$$Q_{\text{total}} = \delta Q_{\text{sticking}} + (1-\delta) Q_{\text{sliding}} = \frac{2}{3}\pi\omega\left[\delta\tau_{\text{yield}} + (1-\delta)\mu p\right] \times \left[\left(R_{\text{shoulder}}^3 - R_{\text{probe}}^3\right)(1-\tan\alpha) + R_{\text{probe}}^3 + 3R_{\text{probe}}^2 H\right] \tag{4}$$

which employs a linear weighting of the contribution from sliding and sticking, respectively, in terms of the state variable δ (zero for full sliding and one for full sticking).

4 Evolution of mechanical properties during FSW of Al alloys

The mechanical properties will in general be changed due to the metallurgical evolution during the welding process as well as the subsequent cooling. This is also the case for FSW of heat-treatable Al alloys in which the softening is closely related to the volume fraction, the size and the phase of the hardening precipitates in the alloy which in turn will be affected by the level of temperature as well as the holding time at elevated temperatures. Basically, this is modelled in literature with two types of models. The first type expresses the volume fraction of the hardening precipitates via relatively simple kinetics of precipitate dissolution [40, 41] often referred to as the Myhr and Grong model. This has been applied to FSW by several authors [18, 32, 42, 76]. The basis of the Myhr and Grong model is experiments in which samples are put into an oven and kept there for a specified period of time at a specified temperature. Following this, the samples are mechanically tested for hardness from which curves for hardness vs. thermal history are constructed. The model then relates the fraction of dissolved hardening precipitates X_{d} to the equivalent time of heat treatment, $t_{\text{eq}} = t/t^*$ (where t is the period of time at a temperature T and t^* is the time for total precipitation dissolution at this temperature), in the following way:

$$X_{\text{d}} = t_{\text{eq}}^n \qquad t_{\text{eq}} = \sum_{i=1}^{N_{\text{total}}} \frac{\Delta t_i}{t_i^*} = \sum_{i=1}^{N_{\text{total}}} \frac{\Delta t_i}{t_{\text{ref}} \exp\left[\frac{Q_{\text{eff}}}{R}\left(\frac{1}{T_i} - \frac{1}{T_{\text{ref}}}\right)\right]} \tag{5}$$

where t_{ref} is the time for total dissolution at the reference temperature T_{ref}, R is the gas constant and Q is the effective

activation energy for precipitate dissolution. Equation (6, right) reflects that the equivalent time in a numerical model is found by discretizing the thermal history into small steps, calculating the equivalent time for each step and then summing up in order to find the total equivalent time. The fraction of hardening precipitates f/f_0 then relates to the equivalent time t_{eq} via the fraction of dissolved precipitates X_d in the following manner:

$$\frac{f}{f_0} = 1 - X_d = 1 - t_{eq}^n = 1 - \sqrt{t_{eq}} \tag{6}$$

where n is a material constant which is obtained experimentally. A value of 0.5 is often used as indicated in the last part of Eq. (6). Finally, the hardness distribution is predicted via linear interpolation between the original state and the fully dissolved state, i.e.

$$\mathrm{HV} = (\mathrm{HV_{max}} - \mathrm{HV_{min}})\frac{f}{f_0} + \mathrm{HV_{min}} \tag{7}$$

where $\mathrm{HV_{max}}$ is the hardness of the material in fully hardened condition and $\mathrm{HV_{min}}$ is the hardness of the fully softened (original) material. Some authors have used this model for FSW, and in Fig. 4, resulting hardness profiles from Feng et al. [18] for a "high" welding speed corresponding to "cold" welding conditions are shown for FSW of AL6061-T6. Note that the effect of natural ageing gives some strength recovery as expected, but it has very little effect on residual stresses according to Feng et al. [18].

The effect of including the Myhr and Grong softening model for prediction of residual stresses in AA2024T3 was investigated by Sonne et al. [76]. Here, it was concluded that prediction of the residual stress field could be improved significantly by including the metallurgical model under hot welding conditions.

The second approach of modelling the material softening is more complex and involves the nucleation of precipitates, their growth, coarsening and dissolution in a coupled manner. This type of model is often referred to as the Wagner-Kampmann model originating from the original work [43]. Some examples of application of this model to FSW are given by Robson et al. [44] and Gallais et al. [45].

5 Thermomechanical models for FSW without material flow

A very convenient assumption used by many authors in literature for modelling of residual stresses in FSW is to neglect the material flow during welding. In essence, this normally results in semi-coupled thermomechanical models in a Lagrangian frame, meaning that the thermal field somehow is calculated prior to the mechanical field either by separating

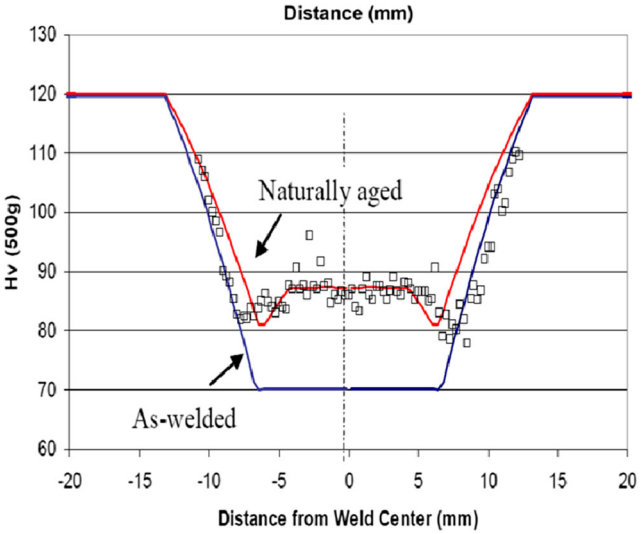

Fig. 4 Microhardness profiles at the mid depth for a FS weld plate of Al6061-T6. *Dots* indicate measurements (naturally aged only) and *lines* indicate modelling results. From Feng et al. [18]

the two analyses totally, i.e. calculating the entire temperature history first and then applying it in the subsequent mechanical analysis, or keeping the separation within the local timestep such that the temperature field is calculated first and the mechanical analysis follows. Both approaches give the possibility of using temperature-dependent material data in the mechanical analysis. These data may come from simple "look-up tables" which are known prior to the thermal analysis and hence are history independent or from models for the evolution of mechanical properties, typically based on microstructural models as described in Section 4.

It is important to underline that the term "semi-coupled" in this context refers to models where the flow during welding is not modelled and the thermal field is addressed by models like the ones presented in Section 3. In this case, the Lagrangian equations in Table 1 for energy and momentum will reduce to the heat conduction equation and the quasi-static equilibrium equations

$$\rho c_p \dot{T} = \left(kT_{,i}\right)_{,i} \quad \sigma_{ji,j} + p_i = 0 \tag{8}$$

These should be solved together with Hooke's generalized law, time-independent plasticity theory and small strain theory i.e. (note that the yield stress in this case only depends on temperature and total equivalent plastic strain) (Table 2).

Several authors in literature have used semi-coupled thermomechanical models without taking material flow into account. The first to do this were Chao and Qi [26] who presented a 3D model in an in-house developed code (predecessor of WELDSIM) with 1800 elements in 1998. This model was pretty advanced for its day because it employed fixture release as well as a history-dependent yield stress such that cooling down would follow a lower curve as compared to

Table 2 Governing equations for semi-coupled thermomechanical models based on computational solid mechanics [35]

$\varepsilon_{ij}^{tot}=\varepsilon_{ij}^{el}+\varepsilon_{ij}^{pl}+\delta_{ij}\varepsilon^{th}$	$\sigma_{ij}=C_{ijkl}(\varepsilon_{ij}^{tot}-\varepsilon_{ij}^{pl}-\delta_{ij}\varepsilon^{th})$	(9)
$C_{ijkl}=\frac{E}{1+\nu}\left(\frac{1}{2}\left(\delta_{ik}\delta_{jl}+\delta_{il}\delta_{jk}\right)+\frac{\nu}{1-2\nu}\delta_{ij}\delta_{kl}\right)$	$\varepsilon_{ij}^{tot}=\frac{1}{2}\left(u_{i,j}+u_{j,i}\right)$	
$\varepsilon^{th}(T_1\rightarrow T_2)=\int_{T_1}^{T_2}\alpha(T)dT$	$\dot{\varepsilon}_{ij}^{pl}=\dot{\lambda}\frac{3}{2}\frac{s_{ij}}{\bar{\sigma}}$	
$\bar{\sigma}=\left(\frac{3}{2}s_{ij}s_{ij}\right)^{\frac{1}{2}}$	$\bar{\varepsilon}^{pl}=\left(\frac{2}{3}\varepsilon_{ij}^{pl}\varepsilon_{ij}^{pl}\right)^{\frac{1}{2}}$	
$f\left(s_{ij},\bar{\varepsilon}^{pl},T\right)=\frac{3}{2}s_{ij}s_{ij}-\sigma_Y^2\left(\bar{\varepsilon}^{pl},T\right)$	$\sigma_Y=\sigma_Y\left(\bar{\varepsilon}^{pl},T\right)$	

heating up. This way, some of the effects of material softening can be captured. Chao and Qi's model was an important step forward, and all models that have followed somehow are based on or inspired by this model.

Feng et al. [18] present an integrated 3D thermal-metallurgical-mechanical model and apply it for predicting the formation of the residual stress field, dissolution of precipitates and ageing in an Al6061-T6 plate which has been friction stir welded. The tool pressure has been taken into account. Simulated residual stress fields for two welding speeds, i.e. 280 mm/min (4.66 mm/s) and 787 mm/min (13.12 mm/s), were compared, and it was found that the low heat input associated with the high welding speed (cold weld) results in higher tensile residual stresses in the weld region. On the other hand, the position of peak tensile residual stress was closer to the weld centre line (narrower tensile zone in the weld). Feng et al. explained this by the less HAZ softening in Al6061-T6 in the high welding speed case. Similar results are found by Bastier et al. [30] who, however, employed a thermal-metallurgical-mechanical model with kinematic hardening *which takes also flow into account*; see Section 6. Chen and Kovacevic [29] as well as Tutum and Hattel [33] (see Fig. 5) also predict higher peak residual stresses however again positioned closer to the weld line (narrower tensile zone) *without* employing a metallurgical model for thermal softening but only a temperature-dependent yield stress in combination with *kinematic* hardening.

So, this effect can also be attributed to the steeper thermal gradients that are present for colder welding conditions provided combined with kinematic hardening. In this context, it is important to emphasize that Zhu and Chao [46] state that the temperature-dependent yield stress is the most governing single parameter for formation of residual stresses in welding simulation. Experimental confirmations of the narrowing effect with higher stress peaks for colder welding conditions are given by, e.g. Wang et al. [16] and Feng et al. [18]. Finally, it should be mentioned that Dubourg et al. [34] find the opposite trend such that higher welding speeds lead to lower residual stresses although they claim that there are some inaccuracies in their model, leading to unrealistic results.

An overview of some of the most important semi-coupled residual stress models without flow in literature for FSW is given in Table 3.

6 Thermomechanical models for FSW with material flow

First of all, it should be emphasized that the main purpose of fully coupled thermomechanical models normally is to get a realistic prediction of the closely coupled material flow, heat generation and temperature fields during welding; see Fig. 2, left. So, seen from that viewpoint, the flow models are normally not intended directly to predict residual stresses themselves. They are normally used as a means of providing more realistic temperature fields and mechanical properties to the subsequent residual stress calculation as compared to what the semi-coupled models are capable of. Flow models for FSW are based on either CFD (computational fluid dynamics) or CSM (computational solid mechanics). Whereas the former are normally not able to predict residual stresses without being coupled to a subsequent residual stress analysis based on CSM, the latter type of models have the potential of predicting residual stresses themselves.

Fully coupled CSM-based flow models for FSW are typically developed from two different approaches: The simplest is to assume a rigid-viscoplastic material—hence, the total strain is equal to the viscoplastic strain and the stress depends on strain rate only—and then typically use an implicit solver

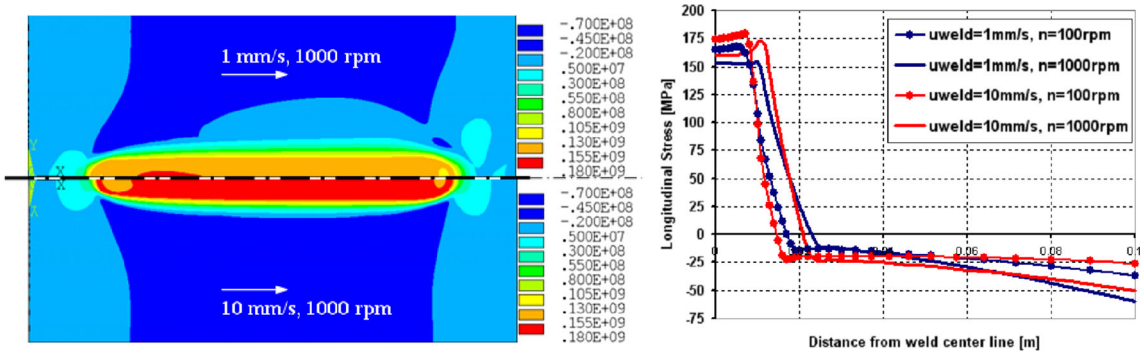

Fig. 5 **a** Contour plot of the longitudinal stress field with increments of 22 MPa [33]. **b** Residual normal stress in longitudinal direction as a function of distance from the weld line [33]

Table 3 Selected thermomechanical models for residual stresses neglecting material flow in FSW

Authors	Year	Formulation			Metallurg. model	Software
		Frame	Solver	Hardening		
Chao and Qi [26]	1999	Lagrangian	Implicit	Isotropic	No	WELDSIM (predass.)
Shi et al. [27]	2003	Lagrangian	Implicit	Isotropic	No	ABAQUS/Standard
Zhu and Chao [28]	2004	Lagrangian	Implicit	Isotropic	No	WELDSIM
Chen and Kovacevic [29]	2006	Lagrangian	Implicit	Kinematic	No	ANSYS
Bastier et al. [30]	2006	Lagrangian	Implicit	Kinematic	Yes	CAST3M
Li et al. [31]	2007	Lagrangian	Implicit	Isotropic	No	ABAQUS/Standard
Feng et al. [18]	2007	Lagrangian	Implicit	Isotropic	Yes	ABAQUS/Standard
Richards et al. [32]	2008	Lagrangian	Implicit	Isotropic	Yes	ABAQUS/Standard
Tutum et al. [8]	2008	Lagrangian	Implicit	Isotropic	No	ABAQUS/Standard
Tutum and Hattel [33]	2010	Lagrangian	Implicit	Kinematic	No	ANSYS
Dubourg et al. [34]	2010	Lagrangian	Implicit	Isotropic	No	LS-DYNA
Carney et al. [71]	2011	Lagrangian	Implicit	Isotropic	No	LS-DYNA
Yan et al. [73]	2011	Lagrangian	Implicit	Isotropic	No	ABAQUS/Standard
Hattel et al. [64]	2012	Lagrangian	Implicit	Isotropic	No	ANSYS
Sonne et al. [76]	2013	Lagrangian	Implicit	Isotropic	Yes	ABAQUS/Standard

based on quasi-static equilibrium. This is done by several authors in literature (see, e.g. [47–49]); although being very applicable for flow, these models will not be able to predict residual stresses in a straightforward manner, since the constitutive law predicts that no stresses will be present when the deformation has come to an end. In this respect, these models resemble CFD models very much. If models of this type, however, are to predict residual stresses, it calls for integration along streamlines. The only CSM model doing this till date in literature has been given by Qin and Michaleris [50] who employ Anand's elasto-viscoplastic model (it is thus not only a rigid-viscoplastic model as the above mentioned) in a Eulerian frame and integrate elastic strains along streamlines in order to finally obtain residual stresses. The model has the advantage like other fully coupled thermomechanical models that it takes the flow into account *while* calculating transient stresses, not only via a more realistic temperature field but also via the mechanical effect of the flow itself, and moreover, since it is a Eulerian steady-state model, it is very fast and does not depend on remeshing, etc.

The second more general approach relies on fully coupled thermomechanical models involving a constitutive law where stresses are expressed in terms of *absolute* strains (as well as strain rates like viscoplasticity to get the flow right), which will be able to predict residual stresses if allowed to calculate for a sufficiently long amount of time. However, as earlier mentioned, they are typically not used for this purpose, but for calculating the flow during the welding process and coupling it with the thermal calculation via the dissipation term in the energy equation.

This more comprehensive approach uses the dynamic equilibrium equations and large strain theory and takes *all* the contributions to the strain into account (including the elastic and rate-independent plastic strains, which make residual stress prediction possible) although the viscoplastic part obviously is the dominating contribution *during* the flow. In a Lagrangian frame, the governing equations are now the energy equation with the plastic dissipation term and the dynamic equilibrium equations as given in Table 1, left (compare with the corresponding governing equations for the semi-coupled case expressed by Eq. (8)). Apart from this, the major change as compared to the semi-coupled models without flow, Eq. (9), lies in the fact that large strain theory must be applied; the viscoplastic strain is now taken into account meaning that rate-dependent constitutive equations must be employed, which among others means expressions for the yield stress, such as the Norton power law, the inverse hyperbolic sign expression involving the Zener-Hollomon parameter and the Johnson-Cook expression; see Eq. (10), Table 4.

For CSM-based models, the implementation is typically done in an arbitrary Lagrangian Eulerian (ALE) formulation where the dynamic equilibrium equations are solved in an explicit manner which in essence results in a very simple algorithm but also calls for very small timesteps, which to some extent can be overcome by the use of mass scaling. This approach has been used by several authors; see, e.g. [51–54] and Table 5. A special feature about the model by Schmidt and Hattel [52] (implemented in ABAQUS/Explicit) is that the surface condition between the tool and the matrix is not prescribed but part of the solution itself. This adds to the

Table 4 Changed, important governing equations for thermomechanical models based on CSM taking flow into account (compare with Table 2) [35]

$\varepsilon_{ij}^{tot}=\varepsilon_{ij}^{el}+\varepsilon_{ij}^{pl}+\varepsilon_{ij}^{vp}+\delta_{ij}\varepsilon^{th}$ or $\varepsilon_{ij}^{tot}=\varepsilon_{ij}^{pl}$

$\sigma_Y = \sigma_Y\left(\bar{\varepsilon}^{pl}, \dot{\bar{\varepsilon}}^{pl}, T\right)$

$\varepsilon_{ij}^{tot} = \frac{1}{2}\left(u_{i,j}+u_{j,i}\right)+u_{k,i}u_{k,j}$ (10)

$\sigma_Y \to 0 \quad T \to T_{\text{cut-off}} \approx T_{\text{sol}}$

Norton power law

$\sigma_Y = K\left(\dot{\bar{\varepsilon}}^{pl}\right)^m$

Zener-Hollomon

$\sigma_Y = \frac{1}{\alpha}\sinh^{-1}\left(\frac{Z}{A}\right)^{1/n}$

$Z = \dot{\bar{\varepsilon}}^{pl}e^{Q/RT} \quad m = \frac{\partial \ln\sigma}{\partial \ln\dot{\varepsilon}^{pl}}$

Johnson-Cook

$\sigma_Y = \left(A + B\left(\varepsilon^{pl}\right)^n\right)\left(1 + C\ln\frac{\dot{\bar{\varepsilon}}^{pl}}{\dot{\varepsilon}_0}\right) \times \left(1-\left(\frac{T-T_{\text{ref}}}{T_{\text{sol}}-T_{\text{ref}}}\right)^m\right)$

generality of the model but also to the complexity and hence the need for computational power.

The model has been used to predict among others the plastic strain in the weld which resembles the well-known "flow arm" quite well, being the first model in literature able to predict this.

The model by Hamilton et al. [54] certainly deserves mention in this respect also. As the model by Zhang et al. [53], it is also based on the model by Schmidt and Hattel [52]; however, it addresses the whole welding path and it is eventually able to reach the quasi-steady state which Schmidt and Hattel's original model was not capable of. The next natural step in the development of these coupled thermomechanical models would be to use it for residual stresses by letting it take the cooling sequence into account also. By doing this, modelling of residual stresses of FSW would get substantially more general as compared to the semi-coupled models, since the welding history would be better described in terms of the closely coupled phenomena of flow, temperatures and microstructure evolution during welding. It is important to emphasize that, since this approach takes the *elastic strains* into account *during* welding, the elastic deformation of the "far field" and hence the pressure conditions will be described more realistically as compared to predicting the flow with a CFD model. Another way to achieve this is to couple a local, steady-state flow model in a Eulerian frame during welding with a global, transient, rate-independent residual stress model during welding and cooling. Some few works in literature are

Table 5 Selected thermomechanical models applicable for residual stresses in FSW including flow

Authors	Year	Formulation				Software
		Structure	Flow	Stress	Met. model	
Xu and Deng [51]	2003	Global	CSM-ALE rigid-viscoplastic	CSM-Lagrangian elasto-plastic	No	ABAQUS/Explicit
Schmidt and Hattel [52]	2005	Global	CSM-ALE elasto-plastic-viscoplastic	CSM-ALE elasto-plastic-viscoplastic	No	ABAQUS/Explicit
Zhang and Zhang [53]	2007	Global	CSM-ALE elasto-plastic-viscoplastic	CSM-ALE elasto-plastic-viscoplastic	No	ABAQUS/Explicit
Bastier et al. [55]	2008	Local/global	CFD-Eulerian rigid-viscoplast.	CSM-Lagrangian elasto-plastic	Yes	CAST3M
De Vuyst et al. [57]	2008	Local/global	CSM-Lagrangian rigid-viscoplast	CSM-Lagrangian elasto-plastic	No	MORFEO/SAMCEF
Qin and Michaleris [50]	2009	Global	CSM-Eulerian elasto-plastic-viscoplastic	Integration of elastic strains along streamlines	No	In-house
Hamilton et al. [54]	2010	Global	CSM-ALE elasto-plastic-viscoplastic	CSM-ALE elasto-plastic-viscoplastic	No	ABAQUS/Explicit
Grujicic et al. [56]	2010	Global	CSM-ALE rigid-viscoplastic	CSM-Lagrangian elasto-plastic-viscoplastic	No	ABAQUS/Explicit and Standard
Buffa et al. [70]	2011	Global	CSM-Lagrangian rigid-viscoplastic	CSM-Lagrangian elasto-plastic	No	DEFORM3D/ABAQUS/ Standard
Riahi and Nazari [72]	2011	Global	CSM-ALE elasto-plastic-viscoplastic	CSM-Lagrangian elasto-plastic	No	ABAQUS/Explicit
Jamshidi et al. [74]	2012	Local	CSM-ALE elasto-plastic-viscoplastic	CSM-Lagrangian elasto-plastic	No	ABAQUS/Explicit
Sadeghi et al. [75]	2013	Global	CSM-Lagrangian rigid-viscoplastic	CSM-Lagrangian elasto-plastic	No	DEFORM3D/ABAQUS/ Standard
Nonrani et al. [77]	2014	Global	CFD-Eulerian rigid-viscoplastic	CSM-Eulerian elasto-viscoplastic	No	Comsol

based on this type of coupled approach. A very interesting example of such model is the work by Bastier et al. which also involves a metallurgical model for the evolution of mechanical properties during and after welding. Another interesting example model is the one given by Grujicic et al. [56] in which a coupled thermomechanical model in ABAQUS/Explicit is applied for the flow during FSW of AA5085-H131 followed by a mapping of the results to a quasi-static thermomechanical model without flow in ABAQUS/Standard for calculation of residual stresses. What should be emphasized here is that even though the flow model is of the CSM type, it is a rigid-viscoplastic model (total strain equal to viscoplastic strain) (see Table 4), thus making the flow model resembling CFD flow models. Moreover, it should also be mentioned that Grujicic et al. suggest a version of the Johnson-Cook constitutive law which takes the dynamic recrystallization into account.

Another interesting model to mention is the one by Buffa et al. [70] where the flow is predicted via a CSM model in a Lagrangian frame, applying DEFORM-3D. Here, the finite element flow formulation is adopted with a rigid-viscoplastic constitutive behaviour for the flow. The transient temperature field is then imported into ABAQUS/Standard for the subsequent stress analysis.

An overview of some important coupled thermomechanical models based on solid mechanics involving elastic and plastic strain (making them capable of calculating residual stresses) from literature is given in Table 5.

7 Discussion

Even though modelling of residual stresses in FSW is a highly interesting subject in itself which could easily be addressed by several review articles (as has hopefully been indicated in the former sections), it is at this point appropriate to put the subject into some proper perspective. In this context, it is natural to ask the question: "Now that we to a reasonable extent can predict residual stresses by experimental measurements and modelling means, (i) is it at all possible to reduce them or even get rid of them? and (ii) how do they affect the mechanical performance of our welded structure?" The next sections are devoted to discussing these issues.

7.1 Reduction of residual stresses in FS welds

This field has attracted some attention, and a few important approaches involving thermomechanical modelling described in literature which might be applicable for FSW are briefly summarized in the following. (i) Applying thermal fields prior to or during welding involving both steady-state and transient thermal tensioning has been addressed in [58–60]. Whereas the first is relatively impractical and costly, the second has been shown to work well for reducing residual stresses in welding. In short, the general idea is to apply moving heat sources at each side of the moving tool, thereby reducing the tendency of plastic yielding in compression during welding which is main cause for residual stresses in tension. Designing these heat sources as regards size, intensity, etc. is, however, quite difficult, and regarding this, several contributions have been given in literature where the model by Michaleris et al. [59] who formulated the task as an optimization problem in combination with a thermo-elasto-plastic model is of particular interest for the subject of the present paper. (ii) Mechanical tensioning [32, 61] in which a load is applied uniformly along opposite ends of the plates prior to clamping the parts for welding, so that a uniform tensile stress is maintained in the two butted plates parallel to the weld line. The clamping and tensioning loads are then released after the FSW tool has traversed along the joint line to form the weld. Altenkirch et al. [60] have shown that this global mechanical tensioning during the welding process can greatly reduce the tensile residual stresses in FSW joints. (iii) Surface process treatment such as shot peening or laser shock peening inducing compressive stresses in the surface counteracted by tensile stresses in the interior of the parts have shown to enhance the fatigue resistance in FS welds [62] as well as other mechanical properties [63]. (iv) Post-weld direct rolling (PWDR), where a single roller is applied to roll the top surface of the weld after the weld metal has cooled to room temperature, has also been proven to be an effective way of reducing the residual stresses. In the work by Wen et al. [78], the effectiveness of using PWDR is illustrated with an industrial example of a large integrally stiffened panel, where the distortion was virtually eliminated, as a result of a reduction in residual stresses.

7.2 Coupling residual stress models for FSW with subsequent loading models

As discussed in the former section, it is actually possible to a large degree to reduce residual stresses in FS welds. Even though low residual stresses will always seem preferable in welded structures as a first choice, it is important to emphasize that in order to fully evaluate the effects of residual stresses in a FSW joint, they should somehow be combined with "in-service knowledge", e.g. coming from an in-service load analysis. This, in order to investigate residual stresses work "in the same direction as" or "in the opposite direction as" the loading stresses but also when combined with loading stresses whether resultant stress peaks are obtained in areas with severely reduced mechanical properties. This is of course to some extent always done implicitly when considering the very purpose of the welded joint, whether, for example, it is situated in a dynamically loaded structure thereby being prone to fatigue or it is part of a thin-walled structure with an overall stress state of compression being prone to buckling. Thus,

recently, models for combining residual stresses with modelling of actual load cases have started to emerge. These can in general be categorized into two types: (i) the first in which a test piece "is taken out of the model" and subjected to free boundaries at the side edges, followed by stress relaxation (if modelled as free) and then loading of the test piece like in a uni-axial test in order to obtain the stress-strain curve and (ii) the second in which residual stresses for an entire welded structure are calculated and the structure itself is loaded afterwards to mimic a real loading case for the structure during service. Examples of the first type have been given by Feng et al. [18] on FSW of 6061-T6 where the subse quent uni-axial loading is based on a large-strain FE analysis which predicts that necking will take place where the large gradient in hardness (yield strength) will be located. This is in line with the results of a somewhat similar analysis by Hattel et al. [64] which involves a sequential thermomechanical model for FSW of a model Al alloy in ANSYS combined with an in-house-developed explicit FE code with a Gurson model for damage evolution during the tensioning post to welding. Two extreme constraining cases of the "test piece" are considered, namely one with free boundaries resembling the normal test piece case and one with constrained boundaries, thus to some extent resembling the test piece still sitting in the structure with high residual stresses; see Fig. 6. Note that the high Mises stresses are associated with the localization concentrated around one shoulder width away from the weld line where the variation in hardness has its maximum. The main conclusion of this work is that for both the analysed cases, including the residuals has relatively little effect on the load carrying capacity but reduces ductility considerably.

One example of the second type has been given by Tutum et al. in which the FSW of a stringer on a plate (see Fig. 7a) has been thermomechanically modelled with ABAQUS/Standard to obtain residual stresses and then subsequently subjected to an in-service load also modelled in ABAQUS/Standard; see Fig. 7(b). As seen, applying the load actually slightly reduces the longitudinal stresses in the middle of the weld. This is of course not a general statement but only valid for this geometry and load case; however, it serves to show the value of combining the residual stress analysis with an in-service loading analysis.

7.3 Optimization of FSW based on residual stress modelling

Some examples of using numerical optimization methods in combination with process modelling of FSW have been given in literature. Most of them are based on thermal models, and they are typically targeted at obtaining optimal process parameters with respect to predefined objectives or used as a means of inverse modelling to obtain unknown properties like heat transfer coefficients; a few will be mentioned in the following. Liao and Daftardar [65] use a thermal model in FLUENT in combination with two simpler surrogate models to investigate the performance of different optimization algorithms for obtaining the three process parameters, heat input, weld speed and shoulder diameter. Tutum et al. [66] combine a gradient-based optimization technique (i.e. sequential quadratic programming (SQP)) with a simple analytical thermal model in order to obtain heat input and welding speed for a desirable average temperature distribution under the tool shoulder in the FSW process. The same process criterion is studied using space and manifold mapping by Larsen et al. [67]. An application of the differential evolution algorithm for reducing the uncertainty associated with specific process parameters, i.e. the friction coefficient, the extent of slip between the tool and the workpiece, the heat transfer coefficient at the bottom of the workpiece, the mechanical efficiency and the extent of viscous dissipation converted to heat, is studied by Nandan et al. [68]. It should be mentioned that this application is based on a coupled viscoplastic thermal-flow model for FSW. A recent contribution is given by Tutum et al. [69] who combine a 2D steady-state Eulerian TPM heat source model (see Eqs. (3) and (4)) and an analytically prescribed flow field with a hybrid evolutionary multi-objective optimization algorithm (i.e. NSGA-II and SQP) to find multiple trade-off designs. The only example in literature so far, regarding optimization of FSW based on residual stress calculations, has been given by Tutum and Hattel [33].

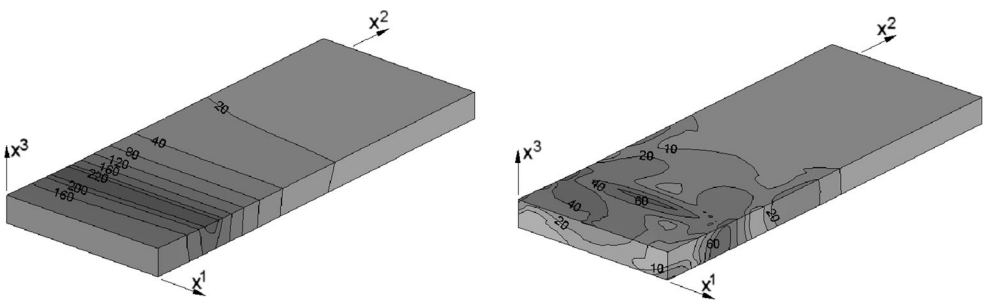

Fig. 6 Predicted Mises stress fields in specimens cut transverse to the weld line. **a** The constrained specimen with zero displacement in the x^1 direction. **b** The relaxed unconstrained specimen with free boundaries. Both with symmetry conditions at the x^1x^3 plane [64]

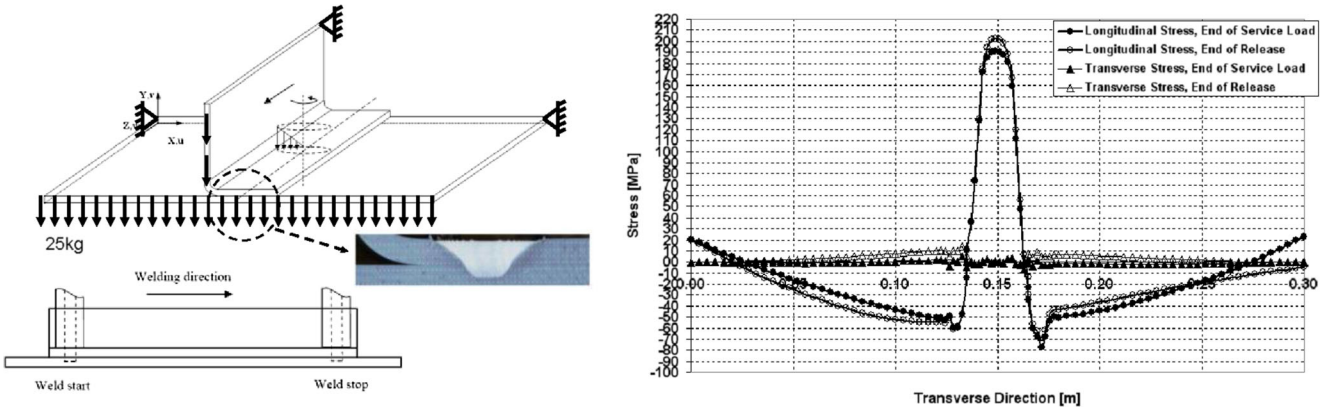

Fig. 7 **a** FSW of a stringer on a plate [8] (courtesy of EADS). **b** Longitudinal and transverse stresses in mid-cross section after releasing and after loading [8]

This work combines a thermomechanical model in ANSYS (neglecting the material flow) with the non-dominating sorting genetic algorithm II (NSGA-II) in order to find optimal values for the welding speed and rotational speed based on an objective of reducing the peak residual longitudinal stress in the weld alongside with increasing the welding speed. This is a multi-objective optimization problem with conflicting objectives, and the corresponding Pareto curve can be seen in Fig. 8. Note that the residual stress curves in Fig. 5b represent some of the stress results from this analysis.

8 Conclusion

Today, residual stresses in FSW of Al alloys are possible to predict with reasonable accuracy by the use of numerical models. Most of the contributions given in literature where comparisons with measurements are given show relatively good agreement regarding the tendencies; however, in some cases, there is somewhat less agreement regarding the absolute levels. In this context, it is again important to mention the point of stress relaxation when preparing test pieces out of the welds.

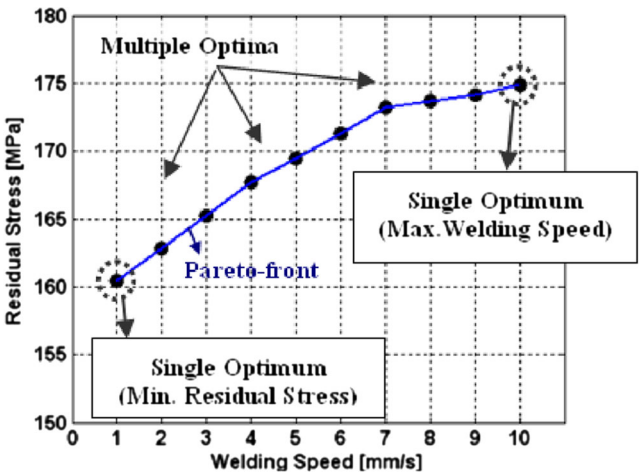

Fig. 8 Pareto line for the optimization case presented in [33]. Note the conflicting objectives of minimizing peak residual stresses alongside with increasing the welding speed

Essentially, a numerical model for residual stresses in FSW must at least comprise a thermal model and a subsequent elasto-plastic mechanical model with a temperature-dependent yield stress. As shown in the paper, this can be improved by coupling with a metallurgical model for the evolution of mechanical properties such as hardness and thereby yield strength and/or by coupling with a model for the flow during welding. Even though adding these two types of additional models to the more rudimentary, pure thermal-mechanical models obviously takes more important physical phenomena into account, it is interesting to note that many authors of the simpler models (without metallurgical and flow models) succeed in predicting the right trends for residual stresses as a function of process parameters as well as reasonable levels as compared to measurements. Models of this type can still serve as "first impression" models in the future; however, it is the firm expectation of the authors that the more complex residual stress models involving both metallurgical and flow models will be increasingly more predominant in the time to come. However, apart from the further development of the residual stress models themselves, it is also very likely that more examples of combining these models with in-service load models for prediction of overall mechanical performance of the welded structures as well as optimization as discussed in Section 6 will be more common in the future so that levels and distributions of residual stresses in FSW will not only be predicted with increasingly improved accuracy but also used to evaluate how the real structures perform during loading, taking residual stresses into account, and how the processes could be optimized in order to improve this performance.

References

1. Mishra RS, Ma ZY (2005) Friction stir welding and processing. Mater Sci Eng A 50:1–78
2. Dalle Donne C, Biallas G, Ghidini T, Raimbeaux G (2000) Effect of weld imperfections and residual stresses on the fatigue crack propagation in friction stir welded joints. 2nd International Conference on Friction Stir Welding. Gothenburg, Sweden
3. Dalle Donne C, Lima E, Wegener E, Pizalla A, Buslaps T (2001) Investigations on residual stresses in friction stir welds. 3rd International Conference on Friction Stir Welding, Kobe, Japan
4. Schindler H-J (1995) Determination of residual stress distribution from measured stress intensity factors. Int J Fract 74:R23–R30
5. Peel M, Steuwer A, Preuss M, P J (2003) Withers, microstructure, mechanical properties and residual stresses as a function of welding speed in aluminum AA5083 friction stir welds. vol 51, Issue 16, pp 4791–4801
6. Staron P, Kocak M, Williams SW, Wescott A (2004) Phys B Condens Matter 350(1–3):E491–E493
7. Reynolds AP, Tang W, Gnaupel-Herold T, Prask H (2003) Structure, properties and residual stress of 304 L stainless steel friction stir welds. Scripta Mater 48(9):1289–1294
8. Tutum CC, Schmidt HB, Hattel J (2008) Assessment of benchmark cases for modeling of residual stresses and distortions in friction stir welding. 7th International Symposium Friction Stir Welding, TWI
9. James MN, Hughes DJ, Chen Z, Lombard H, Hattingh DG, Asquith D, Yates JR, Webster PJ (2007) Residual stresses and fatigue performance. Eng Fail Anal 14:384–395
10. Bussu G, Irving PE (2003) The role of residual stress and heat affected zone properties on fatigue crack propagation in friction stir welded 2024-T351 aluminum joints. Int J Fatigue 25:77–88
11. Murphy A, McCune W, Quinn D, Price M (2007) The characterization of friction stir welding process effects on stiffened panel buckling performance. Thin-Walled Struct 45:339–351
12. Bhide B, Michaleris P, Posoda M, DeLoach J (2006) Comparison of buckling distortion propensity for SAW, GMAW, and FSW. Welding J, 189–195
13. Oosterkamp LD, Webster PJ, Browne PA, Vaughan GBM, Withers PJ (2000) Proc. 5th Eur. Conf. on 'Residual stresses'. Mater Sci Forum 347–349:687–693
14. Webster PJ, Oosterkamp LD, Browne PA, Hughes DJ, Kang WP, Withers PJ, Vaughan GBM (2001) J Strain Anal Eng Design 36:61–70
15. James MN, Hughes DJ, Hattingh DG, Bradley GR, Mills G, Webster PJ (2004) Fatig Fract Eng Mater Struct 27:187–202
16. Wang XL, Feng XL, David SA, Spooner S, Hubbard CR (2000) Proc. 6th Int. Conf. on 'Residual stresses', Oxford, UK, July 2000, IOM
17. Staron P, Kocak M, Williams S (2003) 6th Int. 'Trends in welding research, conference proceedings'. In: David SA et al. (ed), Materials Park, OH, ASM International, pp 253–256
18. Feng Z, Wang X, David SA, Sklad P (2007) Modeling of residual stresses and property distributions in friction stir welds of aluminum alloy 6061-T6. Science and Technology of Welding & Joining 12(4): 348–356, 9
19. Prime MB (1999) Residual stress measurement by successive extension of a slot: the crack compliance method. Appl Mech Rev 52(2): 75–96
20. Ghidini T, Dalle Donne C (2007) Fatig Fract Eng Mater Struct 30: 214–222
21. Mahoney M, Fuller C, DeWald A, Hill MR (2006) Proceedings of 6th International Symposium on 'Friction stir welding', Saint-Sauveur, Montreal, October 2006, TWI, Canada
22. Threadgill PL, Leonard AJ, Shercliff HR, Withers PJ (2009) Friction stir welding of aluminum alloys. vol 54, No:2, Int Mater Rev
23. Prime MB, Gnaupel–Herold T, Baumann JA, Lederich RJ, Bowden DM, Sebring RJ (2006) Acta Mater 54:4013–4021
24. Woo W, Feng Z, Wang XL, Brown DW, Clausen B, An K, Choo H, Hubbard CR, David SA (2007) In situ neutron diffraction measurements of temperature and stresses during friction stir welding of 6061-T6 aluminium alloy. Sci Tech Weld Joining 12(4):298–303
25. dos Santos JF, Kostka A, Fischer T, Staron P, Bergmann L, Huber N, Schreyer A. An in-situ study of precipitation phenomena in AA7449 friction stir welds. 8th International Conference on Friction Stir Welding, Lübeck, Germany
26. Chao YJ, Qi XH (1998) Thermal and thermo-mechanical modeling of friction stir welding of aluminum alloy 6061-T6. J Mater Process Manuf Sci 7(2):215–233
27. Zhu XK, Chao (2004) Numerical simulation of transient temperature and residual stresses in friction stir welding of 304 L stainless steel. J Mater Process Technol 146:263–272
28. Shi Q, Dickerson T, Shercliff H (2003) Proceedings of the 4th International Symposium on FSW, TWI, Utah, USA
29. Chen CM, Kovacevic R (2006) Parametric finite element analysis of stress evolution during friction stir welding. Proceedings of the Institution of Mechanical Engineers Part B: J Eng Manuf 220(8): 1359–1371
30. Bastier A, Maitournam MH, Van KD, Roger F (2006) Sci Technol Weld Join 11:278–288
31. Li T, Shi QY, Li HK (2007) Residual stresses simulation for friction stir welded joint. Sci Technol Weld Join 12(8):634–640
32. Richards DG, Prangnell PB, Williams SW, Withers PJ (2008) Global mechanical tensioning for the management of residual stresses in welds. Mater Sci Eng A; 489(1–2):351–362
33. Tutum CC, Hattel JH (2010) Optimization of process parameters in friction stir welding based on residual stress analysis: a feasibility study. Sci Techn Welding Joining 15(5):369–377
34. Dubourg L, Doran P, Larose S, Gharghouri MA, Jahazi M (2010) Prediction and measurements of thermal residual stresses in AA2024-T3 friction stir welds as a function of welding parameters. Mater Sci Forum 638–642:1215–1220
35. Hattel JH, Schmidt HB, Tutum CC (2008) Thermomechanical modelling of friction stir welding, 8th International Conference on Trends in Welding Research Conference, ASM
36. Tutum CC, Hattel JH (2010) A multi-objective optimization application in friction stir welding: considering thermo-mechanical aspects. IEEE Congress on Evolutionary Computation (IEEE CEC 2010) pp 427–434, 2010, Barcelona, Spain
37. Schmidt H, Hattel J (2005) Modelling heat flow around tool probe in friction stir welding. Sci Technol Weld Join 10(2):176–186
38. Schmidt H, Hattel J (2008) Thermal modelling of friction stir welding. Scr Mater 58:332–337
39. Schmidt H, Hattel J, Wert J (2004) An analytical model for the heat generation in friction stir welding. Model Simul Mater Sci Eng 12(1): 143–157
40. Myhr OR, Grong O (1991) Process modelling applied to 6082-T6 aluminum weldments, part I: reaction kinetics. Acta Mater 39(11): 2693–2702
41. Myhr OR, Grong O (1991) Process modelling applied to 6082-T6 aluminum weldments, part II: applications of model. Acta Mater 39(11):2703–2708
42. Russel M, Shercliff H (1999) Analytical modeling of microstructure development in friction stir welding. 1st International symposium on friction stir welding, USA
43. Wagner R, Kampmann R (1991) Homogeneous second phase precipitation, Weinheim: VCH, Materials science and technology—a comprehensive treatment, Weinheim Volume 5, pp. 213–303
44. Robson JD, Sullivan A, Shercliff HR, McShane G (2004) Microstructural evolution during friction stir welding of AA7449. 5th International symposium on friction stir welding, France

45. Gallais C, Denquin A, Pic A, Simar A, Pardoen T, Brechet Y (2004) Modelling the relationship between process parameters, microstructural evolution and mechanical behaviour in a friction stir welded 6xxx aluminium alloy. 5th International symposium on friction stir welding, France
46. Zhu XK, Chao YJ (2002) Effects of temperature-dependent material properties on welding simulation. Comput Struct 80: 967–976
47. Goetz RL, Jata KV (2001) Modelling friction stir welding of titanium and aluminium alloys. Proc. Symposium on Friction Stir Welding and Processing, TMS
48. Buffa G, Hua J, Shivpuri R, Fratini L (2006) A continuum based fem model for friction stir welding—model development. Mater Sci Eng A 419:389–396
49. Uyyury RK, Kailas SV (2006) Numerical analysis of friction stir welding process. J Mater Eng Perform
50. Qin X, Michaleris P (2009) Thermo-elasto-viscoplastic modelling of friction stir welding. Sci Technol Weld Join 14(7):640–649
51. Xu S, Deng X (2003) Two and three-dimensional finite element models for the friction stir welding process. 4th Int. Symp. On Friction Stir Welding, UT, USA
52. Schmidt H, Hattel J (2005) A local model for the thermomechanical conditions in friction stir welding. Model Simul Mater Sci Eng 13: 77–93
53. Zhang H, Zhang Z (2007) Numerical modelling of friction stir welding process by using rate-dependent constitutive model. J Mater Sci Technol 23(1):73–80
54. Hamilton R, MacKenzie D, Li H (2011) Multi-physics simulation of friction stir welding process. Eng Comput 27(8)
55. Bastier A, Maitournam MH, Roger F, Van Dang K (2008) Modelling of the residual state of friction stir welded plates. J Mater Process Techn 200:25–37
56. Grujicic M, Arakere G, Yalavarthy HV, He T, Yen C-F, Cheeseman BA (2010) Modeling of AA5083 material-microstructure evolution during butt friction stir welding. J Mater Eng Perform 19(5):672–684
57. De Vuyst T, Madhavan V, Ducoeur B, Simar A, de Meester B, D'Alvise L (2008) A thermo-fluid/thermo-mechanical modeling approach for computing temperature cycles and residual stresses in FSW. 7th Int Symp on FSW, Japan
58. Michaleris P, Sun X (1997) Finite element analysis of thermal tensioning techniques mitigating weld buckling distortion. Weld J 76(11):451–457
59. Michaleris P, Dantzig J, Torterelli D (1999) Minimization of welding residual stress and distortion in large structures. Weld J 78:361–366
60. Richards DG, Prangnell PB, Withers PJ, Williams SW, Nagy T, Morgan S (2008) Simulation of the effectiveness of dynamic cooling for controlling residual stresses in friction stir welds. 7th International Symposium Friction Stir Welding, TWI
61. Altenkirch J, Steuwer A, Peel M, Richards DG, Withers PJ (2008) The effect of tensioning and sectioning on residual stresses in aluminum AA7749 friction stir welds. Mater Sci Eng A 488:16–24
62. Hatamleh O, Lyons J, Forman R (2007) Laser and shot peening effects on fatigue crack growth in friction stir welded 7075-T7351 aluminum alloy joints. Int J Fatigue 29(3):421–434
63. Hatamleh O (2008) The effects of laser peening and shot peening on mechanical properties in friction stir welded 7075-T7351 aluminum. J Mater Eng Perform 17:688–694
64. Hattel JH, Nielsen KL, Tutum CC (2012) The effect of post-welding conditions in friction stir welds: from weld simulation to ductile failure. Eur J Mech A/Solids 33:67–74
65. Liao TW, Daftardar S (2009) Model based optimization of friction stir welding processes. Sci Technol Weld Join 14(5):426–435
66. Tutum CC, Schmidt H, Hattel J, Bendsøe M (2007) Estimation of the welding speed and heat input in friction stir welding using thermal models and optimization. 7th World Congress on Structural and Multidisciplinary Optimization, Seoul, pp 2639–2646
67. Larsen AA, Bendsøe MP, Hattel JH, Schmidt HNB (2009) Optimization of friction stir welding using space mapping and manifold mapping—an initial study of thermal aspects. Struct Multidiscip Optim 38(3):289–299
68. Nandan R, Lienert TJ, DebRoy T (2008) Toward reliable calculations of heat and plastic flow during friction stir welding of Ti-6Al-4 V alloy. Int J Mat Res 99(4):434–444
69. Tutum CC, Deb K, Hattel JH (2010) Hybrid search for faster production and safer process conditions in friction stir welding. The Eighth International Conference on Simulated Evolution and Learning (SEAL-2010), December 2010, IITK Kanpur, India (accepted)
70. Buffa G, Ducato A, Fratini L (2011) Numerical procedure for residual stresses prediction in friction stir welding. Finite Elem Anal Des 47: 470–476
71. Carney KS, Hatamleh O, Smith J, Matrka T, Gilat A et al (2011) A numerical simulation of the residual stresses in laser-peened friction stir-welded aluminum 2195 joints. Int J Struct Integ 2(1):62–73
72. Riahi M, Nazari H (2011) Analysis of transient temperature and residual thermal stresses in friction stir welding of aluminum alloy 6061-T6 via numerical simulation. Int J Adv Manuf Technol 55:143–152
73. Yan D, Wu A, Silvanu J, Shi Q (2011) Predicting residual distortion of aluminum alloy stiffened sheet after friction stir welding by numerical simulation. Mater Des 32:2284–2291
74. Jamshidi Aval H, Serajzadeh S, Kokabi AH (2012) Experimental and theoretical evaluations of thermal histories and residual stresses in dissimilar friction stir welding of AA5086-AA6061. Int J Adv Manuf Technol 61:149–160
75. Sadeghi S, Najafabadi MA, Javadi Y, Mohammadisefat M (2013) Using ultrasonic waves and finite element method to evaluate through-thickness residual stresses distribution in the friction stir welding of aluminum plates. Mater Des 52:870–880
76. Sonne MR, Tutum CC, Hattel JH, Simar A, de Meester B (2013) The effect of hardening laws and thermal softening on modeling residual stresses in FSW of aluminum alloy 2024-T3. J Mater Process Technol 213:477–486
77. Nourani M, Milani AS, Yannacopoulos S, Yan CY (2014) Predicting residual stresses in friction stir welding of aluminum alloy 6061 using an integrated multiphysics model. Mater Sci Forum 768–769:682–689
78. Wen SW, Colegrove PA, Williams SW, Morgan SA, Wescott A, Poad M (2010) Rolling to control residual stress and distortion in friction stir welds. Sci Technol Weld Join 15(6):440–447
79. Frigaard Ø, Grong Ø, Midling OT (2001—1189) A process model for friction stir welding of age hardening aluminum alloys. Metallurgical and Materials Transactions A, vol 32a